

## Chitosan nanoparticles containing the insecticide dimethoate: A new approach in the reduction of harmful ecotoxicological effects

José Henrique Vallim <sup>a</sup>, Zaira Clemente <sup>a</sup>, Rodrigo Fernandes Castanha <sup>a</sup>, Anderson do Espírito Santo Pereira <sup>b</sup>, Estefânia Vangelie Ramos Campos <sup>b</sup>, Márcia Regina Assalin <sup>a</sup>, Cláudia Vianna Maurer-Morelli <sup>c</sup>, Leonardo Fernandes Fraceto <sup>b</sup>, Vera Lúcia Scherholz Salgado de Castro <sup>a,\*</sup>

<sup>a</sup> Embrapa Environment, Rod SP 340, km 127.5, 13918-110, Jaguariúna, São Paulo, Brazil

<sup>b</sup> Department of Environmental Engineering, Sorocaba Institute of Science and Technology (ICTS), São Paulo State University (Unesp), Avenida Três de Março, 511, 18087-180, Sorocaba, São Paulo, Brazil

<sup>c</sup> Department of Translational Medicine, School of Medical Sciences, University of Campinas (Unicamp), 13087-883, Campinas, São Paulo, Brazil

### ARTICLE INFO

Editor: Phil Demokritou

**Keywords:**

Sustainability  
Agriculture  
Ecotoxicity  
Nanopesticides  
Chitosan

### ABSTRACT

Organophosphate insecticides such as dimethoate (DMT) are widely used in agriculture. As a side effect, however, these insecticides contaminate bodies of water, resulting in damage to aquatic organisms. The development of nanopesticides may be an innovative alternative in the control of agricultural pests, increasing effectiveness and reducing their toxicological effects. Based upon this, the present study has investigated encapsulated DMT in alginate chitosan nanoparticles (nanoDMT) and evaluated its toxicological effects on non-target organisms. The nanoparticles were characterized by DLS, NTA and AFM, as well as being evaluated by the release profile. Nanoparticle toxicity was also evaluated in comparison with DMT, empty nanoparticles and DMT (NP + DMT), and commercial formulations (cDMT), in the embryos and larvae of *Danio rerio* (zebrafish) according to lethality, morphology, and behavior. The nanoparticle control (NP) showed hydrodynamic size values of  $283 \pm 4$  nm, a PDI of  $0.5 \pm 0.05$  and a zeta potential of  $-31 \pm 0.4$  mV. For nanoparticles containing dimethoate, the nanoparticles showed  $301 \pm 7$  nm size values, a PDI of  $0.45 \pm 0.02$ , a zeta potential of  $-27.9 \pm 0.2$  mV, and an encapsulation of  $75 \pm 0.32\%$ , with slow-release overtime (52% after 48 h). The AFM images showed that both types of nanoparticles showed spherical morphology. Major toxic effects on embryo larval development were observed in commercial dimethoate exposure followed by the technical pesticide, predominantly in the highest tested concentrations. With regard to the toxic effects of sodium alginate/chitosan, although there was an increase for LC<sub>50</sub>–96 h concerning the technical dimethoate, the behavior of the larvae was not affected. The data obtained demonstrate that nanoencapsulated dimethoate reduces the toxicity of insecticides on zebrafish larvae, suggesting that nanoencapsulation may be safer for non-target species, by eliminating collateral effects and thus promoting sustainable agriculture.

### 1. Introduction

Organophosphates (OPs), such as dimethoate, are a class of insecticides, utilized in various regions around the world (Sousa et al., 2018), that can contaminate surface waters due to their extensive applications in urban and agricultural areas (Triassi et al., 2019). The distribution of these insecticides in water is affected by different factors,

such as the groundwater flow field; the OPs used in agricultural activities; and the season, since the ecological risk of OPs to surface water is greater in summer than it is in winter due to sunlight (Wang et al., 2021a; Rani and Sud, 2022). Moreover, a significant risk to non-target organisms, including humans (Hertz-Pannier et al., 2018; Katsikantami et al., 2019) and others, such as fish (Schmitt et al., 2019; Dogan et al., 2011), may occur due to a leaching process in neighboring

**Abbreviations:** DMT, dimethoate; NP, nanoparticle control; nanoDMT, nanoencapsulated dimethoate; cDMT, commercial dimethoate; NP + DMT, nanoparticles plus dimethoate.

\* Corresponding author at: Embrapa Environment, Laboratory of Ecotoxicology and Biosafety, Rod SP 340, km 127.5, 13918-110, Jaguariúna, São Paulo, Brazil.  
E-mail address: [vera-lucia.castro@embrapa.br](mailto:vera-lucia.castro@embrapa.br) (V.L.S. de Castro).

<https://doi.org/10.1016/j.impact.2022.100408>

Received 1 February 2022; Received in revised form 19 May 2022; Accepted 22 May 2022

Available online 31 May 2022

2452-0748/© 2022 Elsevier B.V. All rights reserved.

aquatic ecosystems in a dose and time-dependent form (Nazir et al., 2022).

The dimethoate mechanism of intoxication in mammals is due to the inhibition of acetylcholinesterase (AChE) with a subsequent accumulation of acetylcholine (ACh) in the synaptic cleft, followed by the stimulation of cholinergic receptors (Mesallam et al., 2018). ACh is a neurotransmitter involved in movement and acts as an important modulator of cognitive functions, such as learning and memory (Janeczek et al., 2017; Roy et al., 2017).

However, this enzyme is highly evolutionarily conserved, being present in several tissues of a large number of distinct species, invertebrates, and vertebrates, in aquatic and terrestrial animals (Pereira et al., 2019). ACh is synthesized by practically all living cells from mammals to lower invertebrates, protozoa, plants, fungi, algae, and even bacteria (Toledo-Ibarra et al., 2018).

Moreover, other factors besides the inhibition of AChE influence larval behavior in zebrafish (*Danio rerio*) after exposure to OPs. These pesticides can also cause neurobehavioral effects at low concentrations that are not able to reduce enzyme activity markedly (Schmitt et al., 2019; Aldridge et al., 2005; Eddins et al., 2010). Therefore, the active mechanisms of these insecticides are not entirely clear.

Since OPs can produce several toxic effects, some of which are not yet well determined, a formulation that reduces the pesticide required amount or its release is highly desirable to reduce the environmental risks related to these chemicals. In this context, nanotechnology may be a desirable option to generate a wide variety of new formulations (Slattery et al., 2019) and thereby to improve pesticide efficiency and safety (Zhao et al., 2018). The nanoencapsulation of pesticides can provide a sustained release of the active ingredient while efficiently increasing their stability and solubility, improving their biological activity (Camara et al., 2019). The use of these nanoformulations may then improve crop productivity and decrease harmful effects on the environment (Khandelwal et al., 2016; Kumar et al., 2017; Walker et al., 2018). Such formulations, which alter the risk profile of the active ingredients, are prepared in order to target benefits over conventional products as lower losses of active ingredients through the leaching and evaporation processes (Walker et al., 2018; Kumar et al., 2019; Vurro et al., 2019; Chaud et al., 2021).

According to Kah et al. (2018), the use of nanopesticides can result in an increase of 30% efficiency when compared to non-nano analogs. Conversely, despite evidence of the possible benefits of nanopesticide formulations (Duhan et al., 2017), some concerns persist about their biosafety in their agricultural application (Iavolico et al., 2017; Kah et al., 2018). As for conventional products, there may be a risk to aquatic environments due to the release of the nanopesticide's active principle, resulting in possible toxicity to non-target organisms, the occurrence of bioaccumulation or biomagnification, or interactions with other pollutants in the environment (Walker et al., 2018; Li et al., 2019; Lombi et al., 2019).

Thus, comparisons between toxicological studies of different formulations, such as a commercial one, and those of nanopesticides, can provide additional information for the carrying out of a more complete risk assessment (Kah et al., 2018; Adisa et al., 2019). However, the authors reinforce that biological and toxicological efficacies have not been confirmed for different target flora/fauna in many studies, which means that it cannot be guaranteed that the results will repeat themselves in the field.

Nanocarrier systems based on chitosan have a range of applications for crop protection as delivery systems for pesticides. Nanoparticles of alginate/chitosan have been used as carriers of drugs and agrochemicals in sustained-release systems that can extend the duration of action of the active chemical and improve its stability (Pereira et al., 2017). There is some evidence that avermectin nanoencapsulation with polyamine-modified zein reduces its toxicity to zebrafish and can preserve the pesticide while decreasing toxicity to non-target organisms (Chen et al., 2021). It thus becomes essential – for an understanding of the

environment and fate of the organisms, and for comparisons of the technical and commercial formulations of the active principle – to assess their environmental risks, and as a consequence, to promote safer product development strategies.

The use of zebrafish is a helpful biological platform to investigate the diversity of pesticide-associated toxicity endpoints and therefore their environmental risks. The zebrafish is a vertebrate system model that enjoys substantial acceptance. It has several characteristics that make it suitable for environmental research, such as a low cost, external fertilization, rapid development, transparency (allowing visualization), and genetic homology, all of which are useful in toxicological studies of various chemicals such as nanomaterials. Additionally, there is extensive literature on zebrafish-specific protocols that may be used for toxicological screening (Chakraborty et al., 2016).

Due to these facts, the aim of this study was to develop a nanoformulation for dimethoate based on alginate chitosan particles and evaluate its toxicity in relation to the active ingredient and conventional commercial insecticide formulations, during the embryolarval development of zebrafish, using biochemical and behavioral biomarkers. The formation of the alginate/chitosan complex leads to the formation of more stable materials with a better ability to control chemical release (Pereira et al., 2017; Thai et al., 2020). Then, this study has as an objective the promotion of a new nanoformulation for dimethoate, aiming to reduce its side effects in non-target organisms, and thus to offer a safer alternative for its agricultural use.

## 2. Material and methods

### 2.1. Material

Different formulations of DMT were used in this study i. nanoDMT: encapsulated DMT in alginate chitosan nanoparticles; ii. NP + DMT: empty nanoparticles and DMT (NP and DMT placed separately in the same solution); iii. cDMT: commercial formulation (i.a. 500 g L<sup>-1</sup>); and iv. DMT: technical grade dimethoate (purity of 98.2%).

The dimethoate active ingredient used was Nortox® technical grade (O, O-dimethyl-S methylcarboylmethyl phosphorodithioate) (98.2%) - DMT and the commercial formulation of the OP used was Dimethoate 500 EC Nortox® (500 g.L<sup>-1</sup> - 50.0% w/v) - cDMT. Reagents used for nanoparticle were sodium alginate, CAS 9005-38-3, W201502, Sigma-Aldrich® and chitosan with 80% acetylation, CAS 9012-76-4, 448,869-250G, Sigma-Aldrich®. 3,5-Dichloroaniline >98%, D55792, Sigma-Aldrich® were also used in the fish test as a positive control. The other reagents for embryo medium were purchased from Sigma-Aldrich® or JT Backer®.

### 2.2. Animals

Breeding fish (*D. rerio*, wild-type strain) were kept in laboratory conditions in a zebrafish rack. The water parameters used were conductivity  $400 \pm 0.2 \mu\text{S}$ , a temperature of  $28^\circ\text{C} \pm 0.2$  and a pH of  $7.0 \pm 0.2$ . Conductivity was maintained using Red Sea Salt® and the pH was controlled with acid and alkaline buffers. The *D. rerio* embryos were kept in reconstituted water, prepared according to US EPA (2002). The procedures used in this study were approved by the Ethics Committee on the Use of Animals (CEUA) of the Embrapa Environment protocol n° 003/2015 and University of Campinas (Unicamp, protocol n° 5186-1/2019).

### 2.3. Method for the preparation of alginate/chitosan nanoparticles containing dimethoate

The alginate/chitosan (control) nanoparticles were made using the ionotropic gelation method (Sarmento et al., 2006) with modifications. Firstly, 8 mL of an aqueous solution of sodium alginate at  $0.6 \text{ mg.mL}^{-1}$  was prepared and the pH corrected to 4.9. After this, under magnetic stirring, 2 mL of aqueous calcium chloride solution ( $\text{CaCl}_2 \cdot 2\text{H}_2\text{O}$  - 0.24

$\text{mg.mL}^{-1}$ ) was added slowly, using a peristaltic pump, over 60 min to form a calcium alginate pre-gel forming smaller compact particles. In acidic conditions, alginate maintains a negative charge, an important condition for forming complexes with polyvalent cations that act as bridges between the anionic polymer chains and form a hydrogel network (Loquercio et al., 2015). Subsequently, 2 mL of a chitosan solution (0.24  $\text{mg.mL}^{-1}$  in 0.5% of acetic acid, pH 4.5) was added to the calcium alginate solution. The mixture was stirred using an Ultraturrax (IKA-T25 at 14000 rpm) for 5 min. These nanoparticles are empty (without DMT).

The same protocol above was used for the insecticide-loaded nanoparticle (nanoDMT) preparation. However, 12 mg of DMT was added to the alginate solution until dissolution. The concentration of DMT in this formulation was 1  $\text{mg.mL}^{-1}$ .

#### 2.4. Nanoparticle characterization and stability

##### 2.4.1. Size, polydispersity index and zeta potential

The nanoparticle hydrodynamic size and its distribution (polydispersity index, PDI) were measured using the Dynamic Light Scattering (DLS) technique by Zetasizer Nano ZS90 equipment (Malvern Instruments®, UK). Moreover, zeta potential (mV) values were obtained with the electrophoresis technique using the same equipment. The samples were evaluated in triplicate, without dilution, with light scattering for detection at an angle of 90°, at 25 °C. The same evaluation was performed over different periods in order to assure nanoparticle stability (0, 15, and 30 days). The data were normalized and treated using nonparametric One-Way ANOVA in order to evaluate the nanoparticles' stability overtime.

##### 2.4.2. Size and nanoparticle concentration in the zebrafish embryo medium

To evaluate size distribution and determine the concentration of nanoparticles in the zebrafish embryo medium, the Nanoparticle Tracking Analysis (NTA) technique was applied (equipment ZS90, Malvern Instruments®, UK). For NTA analysis, 10  $\mu\text{L}$  of the NP or nanoDMT was diluted in embryo medium. Each sample was measured 10 times, with an average of approximately 4000 particles. Measurements were performed in triplicate at 25 °C. The hydrodynamic size (nm) and concentration of the nanoparticles ( $\text{particles.mL}^{-1}$ ) were determined by NTA at 0 and 96 h (duration of Fish Embryo Acute Toxicity (FET) test in a zebrafish embryo medium (USEPA, 2002)).

##### 2.4.3. DMT quantification by high pressure liquid Cromatography (HPLC)

The DMT quantification was performed by HPLC using a Varian ProStar instrument, equipped with an OS/210 Pump system, detector UV-Vis OS 325, and Metatherm oven with auto sampler. The stationary column was a Gemini Phenomenex, C<sub>18</sub> (2.6  $\mu\text{m}$  110 A; 250 × 4.60 mm); mobile phase acetonitrile and water were in the proportion of 1:1 (v:v) at a flow of 1  $\text{mL.min}^{-1}$ . The wavelength for detection was  $\lambda = 227 \text{ nm}$ . The determination of the chromatograms was made using the Galaxy Workstation software.

For the construction of the analytical curve, dimethoate stock solutions were prepared in the concentration range from 10 to 60  $\mu\text{g.mL}^{-1}$  and each concentration was submitted to HPLC analysis according to the established chromatographic conditions. Subsequently, a graph of the chromatographic peak area was constructed as a function of the insecticide concentration and the analytical curve was constructed through the linear regression of these data. Three analytical curves were constructed on three consecutive days and the average of these curves was used as a quantitative analysis standard for insecticides ( $r = 0.996$ ). A calibration curve was performed (Fig. A1), and the concentration values were obtained by the equation  $y = 0.88829x + 2.71435$  ( $r = 0.99835$ ), with a detection and quantification limit of 4.16 and 13.89  $\mu\text{g.mL}^{-1}$  respectively.

The DMT stability was measured in the embryo/larvae medium (Fig. A2). The samples were analyzed in duplicate at 0, 5, 24, 48, 72 and

144 h. The concentration values were obtained by the equation  $y = 0.008x + 11.31$  ( $r = 0.872$ ), with a detection and quantification limit of 4.16 and 13.89  $\mu\text{g.mL}^{-1}$  respectively.

The DMT concentration in cDMT and DMT (technical grade) were also measured by equation  $y = 28,201x - 1980.9$  ( $r = 0.9993$ ) and  $y = 28,390x - 1863.8$  ( $r = 0.9987$ ) respectively.

DMT calibration curve by HPLC, DMT stability curve in embryo/larvae medium and concentration plots of DMT (technical grade) and cDMT standard solutions are shown in Material Supplementary (Figs. A1, A2, A3, and A4 respectively).

**2.4.3.1. Encapsulation efficiency.** To evaluate the encapsulation efficiency of nanoDMT, the ultracentrifugation method was utilized. For this, the nanoDMT was centrifuged for 30 min at 200 xg and using Microcon-Millipore® filters with an exclusion pore of 30 kDa. The filtrate was separated to quantify the dimethoate not associated with the nanoparticles through HPLC. To obtain the efficiency of encapsulation, 100% was considered as 1  $\text{mg.mL}^{-1}$ .

##### 2.4.3.2. Release kinetics and the Korsmeyer-Peppas mathematical model.

The DMT release profile from the nanoparticles was evaluated using an *in vitro* system to observe the release profiles of the insecticide nano-encapsulated. The system was composed of two compartments separated by a cellulose membrane with an exclusion pore size of 1 kDa. In the first, the receptor compartment, a solution of  $\text{CaCl}_2$  (11 mM, pH 4.9) was added to deionized water and it was kept under magnetic stirring. In the second, the donor compartment, the insecticide nanoencapsulated and samples were collected as a function of time. The assay was performed in triplicate at room temperature, and the DMT content in the samples was quantified by HPLC (item 2.4.3).

To elucidate the release mechanism, the *Korsmeyer-Peppas* mathematical model was executed (Eq. 1)

$$\frac{M_t}{M_\infty} = ktn \quad (1)$$

Where  $M_t$  is the dimethoate concentration release as a function of time ( $t$ ),  $M_\infty$  the total of dimethoate insert at time 0,  $k$  the kinetic constant, and  $n$  the exponent release. For the mathematical model application, only values below 60% were applied (Siepmann and Peppas, 2001).

##### 2.4.4. Morphology evaluation

The NP and nanoDMT samples were previously dialyzed using a cellulose membrane with 1200 Da molecular exclusion pore (Dialysis Tubing, Sigma®) for 1 h in Milli Q water. The nanoparticles were previously diluted in ultrapure water, in a proportion of 1:10000.

The nanoparticles were previously diluted in a proportion of 1:10000. After that, one drop, approximately 50  $\mu\text{L}$  of the nanoparticles' suspension was deposited onto a silicon chip and allowed to dry at room temperature in a desiccator. The images were obtained using the Nanosurf Easy Scan 2 Basic AFM equipment – pattern BT02217 (Nanosurf®, Switzerland). For scanning the sample in the contact module, TapA1g cantilevers were used (Budget Sensors®, Bulgaria). After the acquisition of the image, at least 100 nanoparticles were manually measured using ImageJ software, to make nanoparticles size distribution histograms.

#### 2.5. Toxicity studies using zebrafish embryo

The embryos of *D. rerio* (3 h post-fertilization – hpf) were exposed to the test conditions for 96 h, according to the OECD 236 (2013) protocol. The exposure was carried out in polystyrene plates of 24 wells ( $n = 24$  organisms per group). The embryos were kept individually in 2 mL of test solution, under a light/dark cycle of 14/10 h at 26.0 ± 0.2 °C in biochemical oxygen demand (BOD) incubator. The positive control was performed with exposure to 4  $\text{mg.L}^{-1}$  of dichloroaniline. The toxicity of

chitosan and alginate alone was also evaluated (10 to 1000 mg.L<sup>-1</sup>).

Preliminary tests were carried out to determine the average lethal concentration (LC<sub>50</sub> mg.L<sup>-1</sup>). The concentrations used to obtain the LC<sub>50</sub> of DMT were 0, 12, 62, 125, 250, 500 and 750 mg.L<sup>-1</sup>, and for cDMT, 0, 2.2, 5, 10, 20, 40, and 80 mg.L<sup>-1</sup>. The following experimental groups were tested at the following concentrations: zero (LC<sub>0</sub> - control embryo medium), LC<sub>10</sub>, LC<sub>20</sub>, LC<sub>30</sub>, LC<sub>40</sub> and LC<sub>50</sub> for the groups NP, nanoDMT, NP + DMT, DMT, and cDMT (commercial dimethoate). The 96 h median lethal concentrations (LC<sub>50</sub>) of the groups tested were calculated for zebrafish embryos. The LC<sub>50</sub> and their 95% confidence intervals were determined by the "Probit Analysis" module of the Statgraphics Centurion XVII program, version 1.17.04, a two-way ANOVA, followed by Bonferroni,  $p < 0.05$ . Following this, estimated LC<sub>40</sub> up to LC<sub>10</sub> of each formulation (technical, commercial or nano) were assessed for comparison of different exposures on the tested biological parameters.

Embryos and larvae were evaluated, after laboratory technician training, every 24 h through a stereomicroscope (SMZ 2 LED, Optika®), to determine the occurrence of malformation and/or mortality. At the end of 96 h in a static medium exposure, live larvae ( $n = 10/\text{group}$ ) were photographed to measure the total length of the larvae using Optika View software, version 7.1.1.5, previously calibrated using a millimeter scale. The larva length (mm) was measured from the head to the tip of the tail. Total larva length was analyzed using the Kruskal-Wallis (KW), followed by the Bonferroni test,  $p < 0.05$ .

Mortality was established as the presence of coagulation, lack of heartbeat, failure to develop somites, and an undisclosed tail. The hatching rate was calculated as the relation between the successful hatching of embryos and the total number of embryos in each replica. The unsteady and irregular movements of the larvae, through visual observation, determined uncoordinated muscle contractions.

Malformations were observed including pericardial edemas, yolk sac edemas, tail deformity, and spinal curvature. Pericardial edema was identified as swelling due to an increase in the volume of fluid in the pericardium (Wu et al., 2019). The presence or absence of an inflated swimming bladder, hypopigmentation beyond column and tail deformities, and alteration in somite formation were determined under a microscope. The percentage of the total number of malformed larvae, in

relation to the total number of larvae that hatched during the test, determined the malformation rate.

## 2.6. Evaluation of behavioral biomarkers in zebrafish larvae (speed and distance covered)

The tests for a behavioral evaluation in zebrafish larvae were performed with DanioVision equipment and analyzed using EthovisionXT software, Noldus®. In 96-well polystyrene plates, 36 larvae/groups were individually distributed per well in a solution of 100  $\mu\text{L}$  embryo medium and 100  $\mu\text{L}$  tested concentration (total volume 200  $\mu\text{L}$ ). Speed (mm.s<sup>-1</sup>) and distance traveled (mm) parameters were evaluated for 10 min at 28 °C ( $n = 36/\text{group}$ ).

The NP, nanoDMT, NP + DMT, DMT, and cDMT were evaluated after 96 h of exposure to LC<sub>10</sub>, LC<sub>20</sub>, and LC<sub>30</sub> concentrations. Organisms exposed to LC<sub>40</sub> and LC<sub>50</sub> were not tested due to mortality. The speed and distance covered by larvae were analyzed using one-way ANOVA followed by the Bonferroni test ( $p < 0.05$ ) considering the effect of the factors of exposure and concentration, as well as the interaction between them ( $p < 0.05$ ).

## 3. Results and discussion

### 3.1. Physicochemical characterization and stability of sodium alginate/chitosan nanoparticles

The hydrodynamic size of the nanoparticles was determined by DLS in order to evaluate nanoparticle characteristics and stability overtime (Fig. 1a). The initial mean diameter of control nanoparticles (NP) was  $282 \pm 4$  nm and a gradual and significant increase was observed as a function of time, and after 30 days the average diameter was  $465 \pm 8$  nm. The polydispersity index (Fig. 1b) of this formulation at the initial time was  $0.57 \pm 0.05$ , followed by a significant decrease of this parameter after 15 days of storage, showing a narrower size distribution (Fig. 1d) and after 30 days there was an increase in PDI to  $0.48 \pm 0.05$ . The initial zeta potential (Fig. 1c) of the nanoparticles was  $-31 \pm 0.5$  mV followed by a significant decrease in the function of storage time.

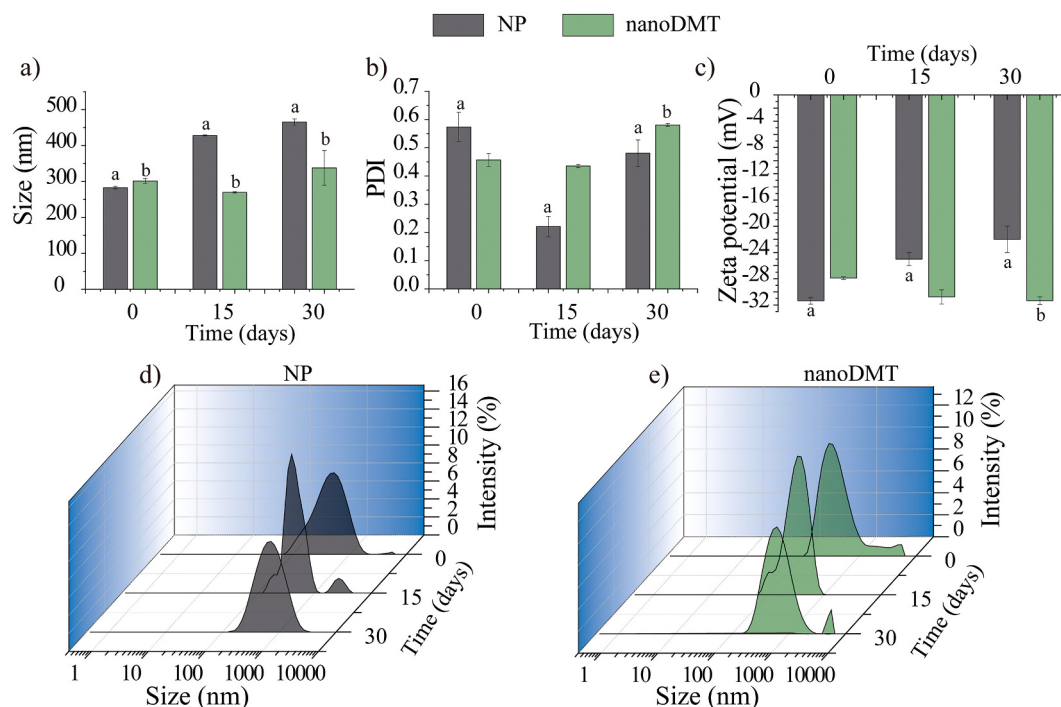


**Fig. 1.** Nanoparticle characterization. NP and nanoDMT were evaluated in relation to: a) hydrodynamic size (nm), b) PDI, c) zeta potential (mV), d) and e) the size distribution of NP and nanoDMT respectively, over time (0, 15 and 30 days). For DLS, the samples were analyzed in triplicate at 25 °C.

For nanoDMT, the initial mean diameter (Fig. 1a) was  $301 \pm 7$  nm, which was bigger than NP at the same time. After 15 days of storage, it was observed a significant decrease in the mean diameter, but after 30 days the size increased again, reaching a value close to the initial average diameter of  $326 \pm 8$  nm. This formulation showed a PDI of  $0.45 \pm 0.02$  (Fig. 1b) and did not show significant changes up to 15 days of storage and after 30 days it was observed a significant increase in this parameter. The change in the nanoparticles stability overtime is a result of homoaggregation, in which the same nanoparticle collides one with another; this can be represented by the PDI increment in Fig. 2b. This effect results in the reduction of surface area availability. As a consequence, in the environment, this effect may reduce nanoparticles toxicity effects (Lowry et al., 2012). The zeta potential (Fig. 1c) of this formulation was  $-27.9 \pm 0.2$  mV and a significant increase after 30 days of storage was observed ( $-31 \pm 0.7$  mV). In addition, for nanoDMT the encapsulation efficiency was evaluated, the nanoparticles were able to encapsulate  $75 \pm 0.32\%$  of the DM and there is no significant difference in encapsulation efficiency over time.

The process of nanoparticle formation, as well as the encapsulation process, occurs through electrostatic interaction, in which the methodology applied and polymer characteristics (molecular weight, number of functional groups), pH, and concentration will determine nanoparticle characteristics (Luo et al., 2020). The composition and nano-preparation method are some determinants of the mean diameter and the polydispersity of the particles (Sharma et al., 2016). According to Luo et al. (2020), the formulation of monodispersed alginate nanoparticles with small particle sizes is difficult to obtain because different alginate sources vary remarkably in their molecular weight, viscosity, and composition. Also, chitosan and alginate molecules form a single larger particle with an increase in their molecular weight ratios.

The nanoparticles produced in this study show high polydispersity (PDI > 0.2); and although the addition of DMT reduced the PDI value, the formulation still has a high polydispersity. Although lower PDI indicates good dispersibility, and as a consequence, good stability (Danaei

et al., 2018), this characteristic of high polydispersity is normal for formulations based on polysaccharides (Pereira et al., 2017) since it is difficult to control the particle size distribution without considering the composition of the nanocarriers and the nature of the solvents used during their preparation. Besides, the high PDI could be explained by the size distribution pattern since a bimodal size distribution was observed from the first day of analysis of the NP and nanoDMT formulations (Figs. 1 d and e). In addition, in a study of alginate/chitosan nanoparticles response surface optimization, the PDI observed for the different nanoparticles produced was between 0.40 and 0.86. Therefore, pH influences alginate reaction with chitosan. At lower pH values, smaller sizes are formed which are more monodisperse (Zohri et al., 2020).

The nanoparticles showed a zeta potential negative, which suggests the presence of carboxylic groups from alginate under the nanoparticle surface (Chen et al., 2019) since negative zeta potential is typically obtained from alginate/chitosan nanoparticles in which the concentration of alginate is bigger than chitosan. The same behavior was not observed for NP, in which the nanoparticles increased in size and PDI with the passage of experimental time (15 and 30 days), which may be a result of the aggregation process. However, each material will grow depending on its reaction conditions (Thanh et al., 2014). Moreover, nanoparticle size growth control during nanopesticide storage is still a great challenge (Lu et al., 2021; Wang et al., 2021b).

The control nanoparticles increase in the mean diameter and PDI, combined with a decrease in the zeta potential value, indicating a stability loss of these formulations and a possible formation of aggregates. Indeed, after 30 days, it can be seen that the size distribution for these nanoparticles (Fig. 1d) is less intense and wider, indicating a possible formation of aggregates. In addition, the zeta potential decrease indicates the main stabilization mechanism of these nanoparticles.

Atomic force microscopy (AFM) was used as a complementary technique to characterize the size of the nanoformulation. Whereas in the DLS technique it was measured the hydrodynamic nanoparticles'

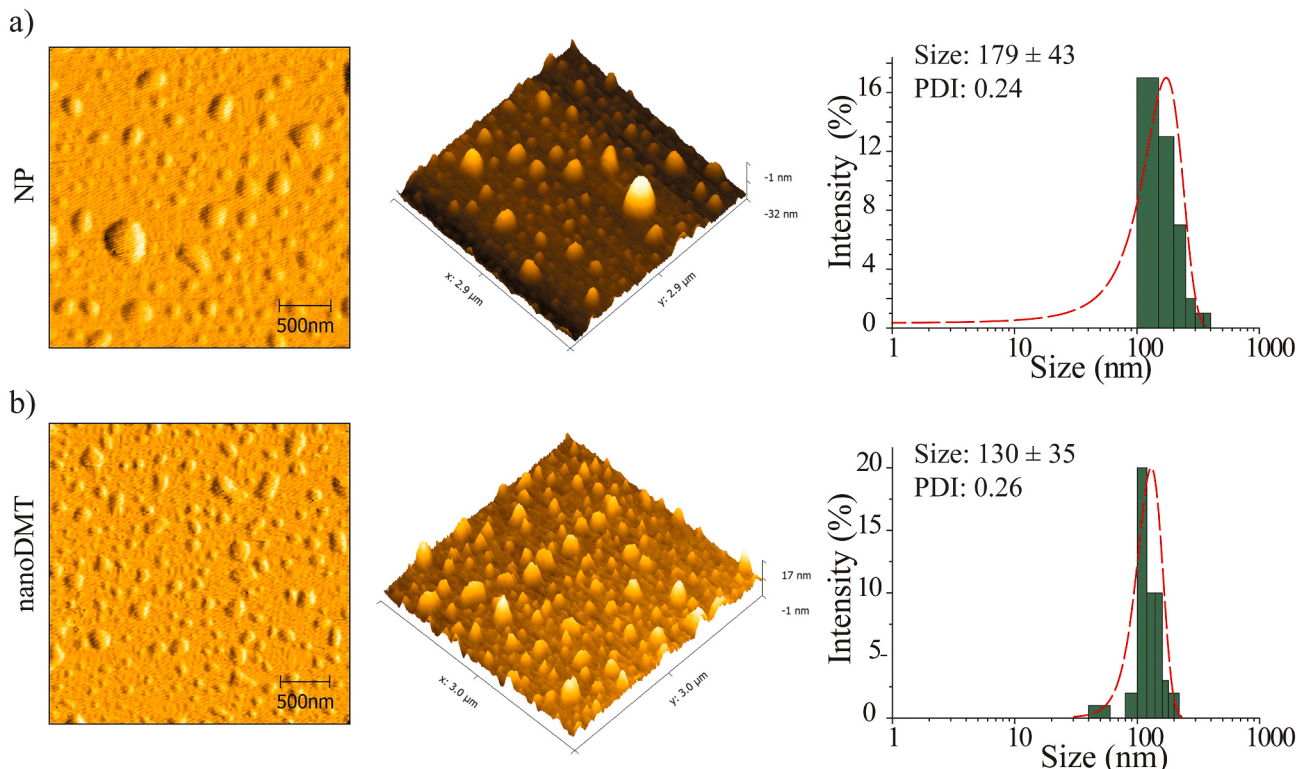


**Fig. 2.** AFM images of NP (a) and nanoDMT (b) respectively (topography, 3D maps and size distribution from left to right). For an evaluation of the size distribution of the AFM image, 100 nanoparticles were counted using the Image J software.

mean diameter; in the AFM analysis, the nanoparticles were deposited on the silicon substrate and dried. The AFM images (Figs. 2 a and b) showed that the nanoparticles have spherical morphology, and according to the distribution graphics, the NP and nanoDMT are  $179 \pm 43$  nm and  $130 \pm 35$  nm in size, respectively. The drying process can explain this reduction in size in comparison with the DLS results during sample preparation. Beyond that, it is worth mentioning that through AFM images, it was possible to observe the nanoparticles' polydispersion, which allows for identifying nanoparticles of different sizes.

### 3.1.1. Release profile evaluation of nanoDMT

The release kinetics were performed in order to demonstrate the DMT release profile (%) in relation to time and the Korsmeyer-Peppas mathematical model (Figs. 3 a and b). The nanoparticles started with a burst release of 25% at 0 h and 5 h; the system released 52% of DMT, staying in this condition until 48 h had passed. The Korsmeyer-Peppas mathematical model demonstrated that the kinetic constant is of  $0.52 \text{ min}^{-1}$ , and the release exponent, 0.09, which represents that the mechanism of dimethoate release from the nanoparticles is by diffusion.

## 3.2. Toxicity studies using the zebrafish model

### 3.2.1. Nanoparticle evaluation in the embryo and larva media

NTA analyses were performed in order to evaluate nanoDMT characteristics (size) and concentration (nanoparticles.mL<sup>-1</sup>) over time (0 h and after 96 h) in the embryo medium for zebrafish. The nanoparticles displayed a hydrodynamic size of  $296.2 \pm 18.1$  nm, corroborating the

results performed by DLS, as in both techniques the hydrodynamic size is measured. The nanoDMT showed no changes in relation to hydrodynamic size over time, however, there is a reduction in nanoparticle concentration from  $2.44 \times 10^{10} \pm 1.62 \times 10^{10}$  to  $1.77 \times 10^{10} \pm 1.31 \times 10^{10}$  nanoparticles.mL<sup>-1</sup> after 96 h. This can be explained by nanoparticle interaction with the zebrafish aquarium medium, which can both result in a hetero-aggregation process, in which the nanoparticles interact with other molecules, increasing in size and resulting in precipitation (Lowry et al., 2012) (Table A1).

### 3.2.2. Toxic evaluation in zebrafish embryos

The organisms were exposed to the negative control (embryo medium) and NP, nanoDMT, NP + DMT, DMT, and cDMT. The organisms of the negative control group (CTL) did not show mortality after 96 h of exposure while the embryo mortality in the group exposed to dichloroaniline (positive control) was 100% after 24 h of exposure. These data validate the tests performed (OECD, 1992, 2013). Zebrafish embryos were exposed to different concentrations of alginate and chitosan alone for 96 h. Both polymers did not cause any mortality even at the highest dose tested. Fig. 4 shows the values obtained for the LC<sub>50</sub>, LC<sub>40</sub>, LC<sub>30</sub>, LC<sub>20</sub>, and LC<sub>10</sub> (mg.L<sup>-1</sup>) of the organisms exposed in the different groups for 96 h.

The results shown in Table A2 reveal that NP did not show toxic effects in zebrafish embryos subjected to different concentrations. The nanoDMT showed less toxicity to organisms since the LC<sub>50</sub>–96 h was statically different from those obtained for organisms in the groups NP + DMT, DMT and cDMT (one-way ANOVA followed by the Bonferroni test,  $p < 0.05$ ). The LC<sub>50</sub>–96 h for nanoDMT was 1.62 times greater than that obtained for DMT, and 52 times greater in relation to cDMT; DMT displayed an LC<sub>50</sub>–96 h 32 times higher than cDMT (Fig. 4 a). The NP + DMT did not show a difference between DMT, indicating that NP cannot result in a synergistic effect (increasing toxic effects) or even protect the embryos from the toxicological effects of DMT. The same behavior is notable for LC 40, 30, and 20, where the LC of nanoDMT was higher than that of DMT or cDMT, which demonstrated that the incorporation of DMT by the nanoparticles is an effective way to reduce side effects in non-target organisms such as zebrafish.

Since the use of conventional pesticide formulations can cause various toxicological issues, improvements in these formulas can reduce their adverse effects on the environment. To that end, the use of nanotechnology to produce new formulations has been shown to be a positive alternative for improving the effectiveness and safety of pesticides (Zhao et al., 2018). A *Danio rerio* development study provides a quick approach to assess the environmental risk of compounds and nanomaterials, and their morphometry is considered a useful assessment in the study of the sub-lethal effects of environmental pollutants (Shaw et al., 2016).

Table 1 represents the mortality and malformation rates for the groups tested and data regarding the changes found in the organisms at 96 h of exposure ( $n = 24$ ). During the LC<sub>50</sub> estimate, although DMT was less toxic than cDMT, it showed 4% mortality at  $62 \text{ mg.L}^{-1}$ . DMT at higher concentrations, such as  $250 \text{ mg.L}^{-1}$ , caused an 87.5% mortality rate in the organisms 72 h post-fertilization (hp) (Table A2).

The organisms exposed to NP and those from the control group (embryo medium) showed no morphological or hatching rate changes after 96 h of exposure. On the other hand, it was observed that organisms in the groups exposed to nanoDMT, NP + DMT, DMT and cDMT suffered a reduction in their hatching rate, in addition to higher percentages with regard to morphological changes.

The groups exposed to nanoDMT showed malformation only after 96 h of exposure to LC<sub>40</sub> and LC<sub>50</sub> (edema of pericardium and calf opacity, Table 1). The groups exposed to NP + DM at LC<sub>30</sub> showed morphological changes after 48 h of exposure (hypopigmentation, pericardial edema, yolk sac edema), LC<sub>40</sub> and LC<sub>50</sub> (hypopigmentation, pericardial edema, yolk sac edema, spine deformities). After 72 h, malformations were observed in LC<sub>40</sub> (hypopigmentation and pericardial edema) and LC<sub>50</sub> exposure (hypopigmentation and yolk sac absorption).

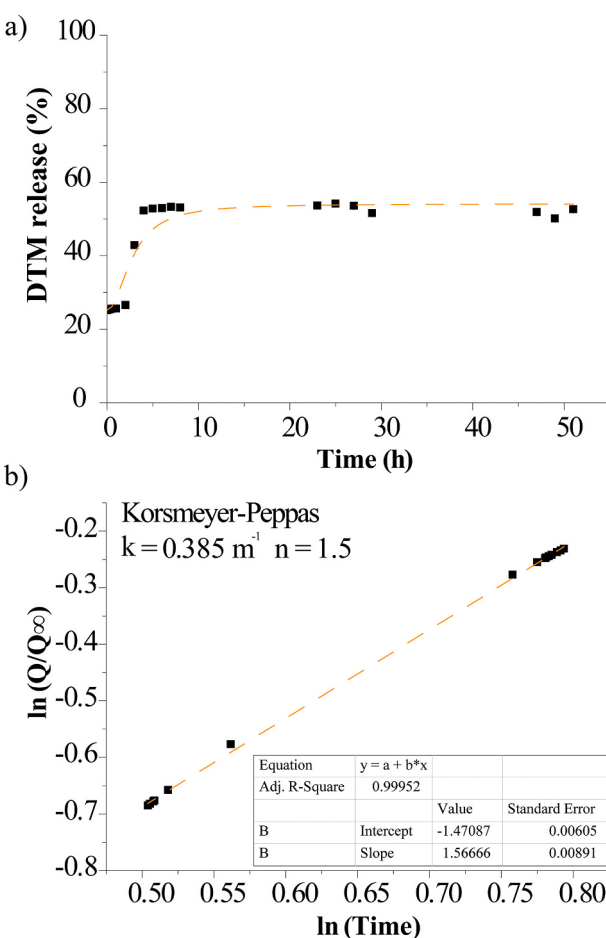
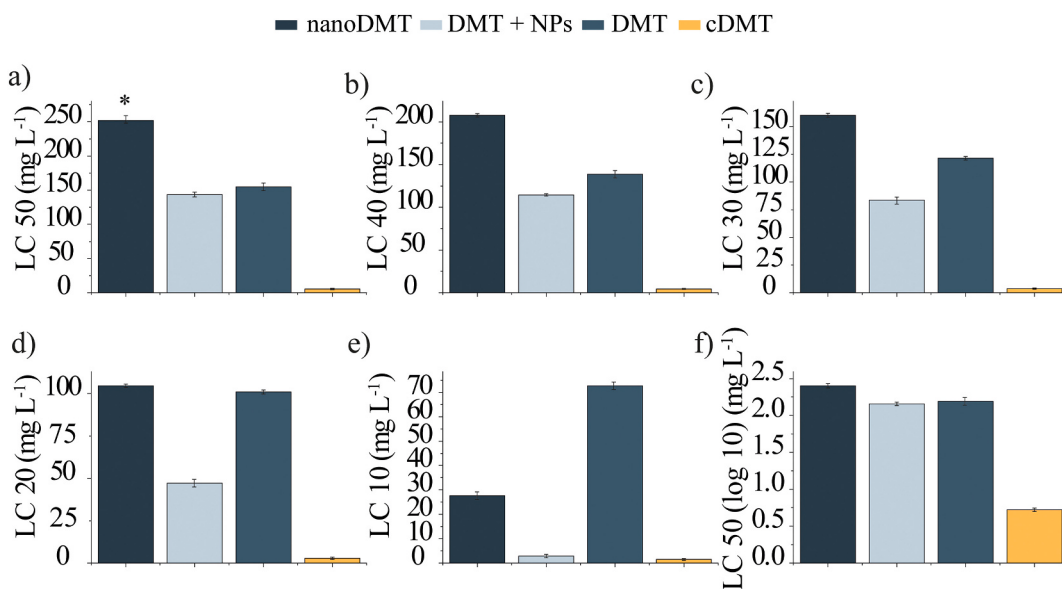


Fig. 3. Kinetic release assay (%) of the asset by nanoparticles ( $n = 3$ ;  $T = 25 \text{ }^{\circ}\text{C}$ ), showing a) the released profile of nanoDMT and b) the Korsmeyer-Peppas mathematical model.



**Fig. 4.** Estimate of LC<sub>10</sub>-LC<sub>50</sub> after zebrafish embryo exposure to different treatments (NP, nanoDMT, NP + DMT, DMT and cDMT), in which a) LC<sub>50</sub>, b) LC<sub>40</sub>, c) LC<sub>30</sub>, d) LC<sub>20</sub>, e) LC<sub>10</sub>, and f) Log<sub>10</sub> of LC<sub>50</sub> for 96 h ( $n = 24/\text{concentration}$ ). The statistical test was made through the “Probit Analysis” module of the Statgraphics Centurion XVII program, version 1.17.04 (Stat Point Technologies, 2014),  $p < 0.05$ .

The groups exposed to DMT showed alterations more quickly after 24 h in LC<sub>40</sub> with regard to pericardial edema. After 72 h of exposure, there were morphological changes in the organisms at all concentrations evaluated according to LC<sub>10</sub> and LC<sub>20</sub> (muscle contractions); LC<sub>30</sub> (muscle contractions, spine/tail deformities and pericardial edema); LC<sub>40</sub> (pericardial edema); and LC<sub>50</sub> (muscle contractions and spinal deformities) (Table 1). For cDMT, after 24 h of exposure, the organisms showed morphological changes at LC<sub>40</sub> (pericardial edema) and LC<sub>50</sub> (muscle contractions). After 48 h of exposure, there were morphological changes in the organisms exposed to LC<sub>10</sub> (spinal deformities), LC<sub>40</sub> (alteration in the formation of somites, tail not detached, hypopigmentation) and LC<sub>50</sub> (edema of pericardium and yolk sac). After 72 h, all tested concentrations promoted damage in the organisms exposed: LC<sub>10</sub> (column/tail deformities and pericardial edema); LC<sub>20</sub> (hypopigmentation); LC<sub>30</sub> (spinal/tail deformities); LC<sub>40</sub> (spinal/tail deformities and pericardial edema) and LC<sub>50</sub> (spinal/tail deformities).

Fig. 5 shows examples of embryonic and larval morphological changes found in the evaluation of zebrafish toxicity in the groups tested.

Consequently, the observations of this study are consistent with abnormalities described in the literature for organophosphate exposure, such as reduction in length (Fraysse et al., 2006). In addition, a decrease in embryonic growth may be due to decreased blood flow and cardiac changes in consequence of a loss of nutrients or problems regarding absorption of nutrients from the yolk sac (Majewski et al., 2018; Qiang et al., 2016; Park et al., 2020). In addition to these possible mechanisms, the inhibition of glucocorticoid synthesis may be related to a delay in the development of the skeletal motor system, since it is important for the stress response and in swimming activity. An increase in cortisol after stress stimulation can occur from 72 hpf, changing homeostatic regulation (Wilson et al., 2013).

Changes, such as pericardial edemas after DMT and cDMT exposure, can be due to cardiovascular abnormalities as a consequence of an increase in the permeability of blood vessels (Hill et al., 2004). The mAChR M2 muscarinic receptors, which are functionally mature at 72 hpf and then sensitive to the effect of AChE (Majewski et al., 2018) can also be involved.

NanoDMT exposure decreased morphological changes in the zebrafish embryos when compared to exposure to the other formulations evaluated in this work, the worst being LC<sub>50</sub>-96 h. The organisms in this

group showed also lower mortality and a higher larval hatching rate.

Thus, it can be noted that nanoDMT caused fewer changes in embryo and larvae than cDMT and DMT. While nanoDMT caused some morphological changes as pericardial edema at LC<sub>40</sub> and LC<sub>50</sub> after 96 h, DMT and cDMT can promote them at 24 h of exposure (pericardial edema) and 72 h (spine/tail deformities and pericardial edema) at lower concentrations. Also, sac yolk edema was observed after 96 h when the organisms were exposed to LC<sub>40</sub> and LC<sub>50</sub> to nanoDMT whereas DMT caused this effect after 48 h. Beyond that, the hatching rate was reduced during the test by DMT exposition in relation to nanoDMT. These facts show that nanoDMT led to fewer morphological changes than conventional formulations and decreased the dimethoate toxicity during zebrafish development.

### 3.3. Evaluation of behavioral biomarkers in zebrafish larvae (speed and distance covered)

The behavioral evaluation of zebrafish larvae at 96 hpf (36 larvae/group) was performed using DanioVision equipment and analyzed through the EthovisionXT software, Noldus®, by observing larva swimming speed (mm·s<sup>-1</sup>) and distance covered (mm) in 10 min at 28 °C. The temperature used was the one considered comfortable for the organisms, without causing stress and the observational time was considered enough to evaluate chemical effects in larvae locomotor as previously determined.

The data were statistically evaluated by Kruskal-Wallis, followed by the Bonferroni test. In general, there was no significant difference in larva swimming velocity or distance covered among the groups. These behavioral biomarkers present some variability due to individual differences among organisms and repeatable individual variation (Hertel et al., 2020).

Some groups presented a behavioral alteration that can be considered a bias, since a dose-response relationship was not found and/or did not present biological significance. Thus, as for velocity measured at LC<sub>30</sub>, the larvae of the NP + DMT group showed a significant difference ( $p < 0.05$ ) from those of DMT and nanoDMT groups (Fig. 6a).

Regarding distance (Fig. 6b), the interaction of the parameter formulation and concentration is considered insignificant ( $p > 0.05$ ), since both did not affect the results.

The evaluation of behavioral parameters did not show significant

**Table 1**  
Evaluation of acute toxicity in zebrafish embryos ( $n = 24$ ) after 96 h of exposure to CTL (control), NP, nanoDMT, NP + DMT, and cDMT at LC<sub>10</sub>, LC<sub>20</sub>, LC<sub>30</sub>, LC<sub>40</sub>, and LC<sub>50</sub> ( $\text{mg L}^{-1}$ ). The data are shown in percentages,  $p < 0.05$ .

% Alterations/ groups	CTL	NP	nanoDMT					NP + DMT					cDMT											
			10	20	30	40	50	10	20	30	40	50	10	20	30	40	50	10	20	30	40	50		
IC 96 h ( $\text{mg L}^{-1}$ )	0	100	100	100	100	93	20	9	6	18	87	36	13	0	26	26	11	27	0	94	90	87	27	13
Hatching rate	100	100	100	100	100	93	20	9	6	18	87	36	13	0	26	26	11	27	0	94	90	87	27	13
Mortality	4	4	4	4	4	11	16	8	37	54	11	20	8	37	16	20	20	25	33	25	16	25	12	20
Pericardium edema	–	–	–	–	–	–	–	–	–	–	–	–	–	–	–	–	–	4	8	8	8	8	8	8
Sac yolk edema	–	–	–	–	–	–	–	–	–	–	–	–	–	–	–	–	–	–	–	–	–	–	–	–
Hypopigmentation	–	–	–	–	–	–	–	–	–	–	–	–	–	–	–	–	–	–	–	–	–	–	–	–
Spinal/rail deformities	–	–	–	–	–	–	–	–	–	–	–	–	–	–	–	–	–	–	–	–	–	–	–	–
Muscle contractions	–	–	–	–	–	–	–	–	–	–	–	–	–	–	–	–	–	–	–	–	–	–	–	–

variations between the groups analyzed and consequently did not affect larva motor development. An organism's locomotive behavior is a parameter of great ecological relevance regarding escape from predators, feeding, and reproduction (Schwalbe et al., 2019). Larva speed and distance traveled present a relationship, since an increase in swimming activity may be due to a stress response or the escape instinct (Ahmad et al., 2012). The swimming performance of foraging fish may remain viable even in the presence of an AChE inhibition compound capable of reducing spontaneous swimming activity such as OPs since the type of muscle used for a given swimming modality appears to correlate with AChE inhibition thresholds (Tierney et al., 2007). Indeed, two OPs, such as chlorpyrifos and malathion may lead to opposite larva behaviors of swimming and rest (Richendrfer and Creton, 2015). Additionally, the organophosphate chlorpyrifos leads to decreased locomotion in zebrafish larvae (Watson et al., 2014; Jin et al., 2015) even after termination of exposure during the embryonic phase (Levin et al., 2004). Besides those above, other effects may be involved in swimming performance, such as cholinergic gene modulation (Clemente et al., 2019) or cholinergic receptor modulation of the conditioned fear and extinction responses (Čolović et al., 2013), among others. Interestingly, embryos can present an increase in locomotion activity after chitosan nanoparticle exposure (Abou-Saleh et al., 2019) although at the time of writing there was no toxicity in concentrations up to  $100 \text{ mg L}^{-1}$ . There will be a need, then, for future studies, in order to elucidate further the dimethoate formulation mechanisms in zebrafish larva behavior.

Since the polymeric nanoparticles of sodium alginate/chitosan with dimethoate displayed less toxicity than with cDMT and DMT, future evaluations should be carried out with the investigation of several biomarkers, the better to understand responses to the exposure of the presently studied dimethoate formulations in zebrafish development.

#### 4. Conclusion

Risk evaluation of agricultural nanopesticide applications is necessary for their correct and safe application. Nanopesticides may have adverse impacts on non-target organisms, which are not properly considered during their development. Consequently, nanosafety information for pesticide risk assessment is still scarce and little is known about the harmful effects of nanopesticides on aquatic vertebrate species.

Because of that, nowadays, the achievement of safer nanoproducts has been the subject of interest. Then, the knowledge obtained from ecotoxicological data is indispensable to make the integration of safety into the innovation process. More than that, it is important to evaluate the environmental risks and potential benefits of nanopesticides relative to conventional formulated pesticides on living organisms.

Ecotoxicology can address environmental risk assessments of nanopesticides through an indicator species monitoring and biomarkers and model organisms used in toxicological assays. In order to study nanopesticide environmental exposures, the zebrafish model has proven itself to be a useful one as a screening tool to determine the risks associated with this exposure. As expected, cDMT was more toxic than DMT and nanoDMT in the tested organisms. In turn, the nanoDMT was a viable alternative in the attempt to decrease toxicity, since it reduced mortality and the number of morphological changes when compared to the other formulations evaluated in this study. There is a need for further studies to seek efficacy in target organisms for nanoDMT, in order to show if the system is able to control insect numbers in low concentrations.

Once a single taxon cannot represent the whole complexity of ecotoxicological effects, the use of different organisms for risk assessment and regulatory decision-making is required. To account for the relevance of the ecotoxicological data in representing the aquatic environment, a species sensitivity distribution (SSD) approach can be used in comparison to pesticide conventional formulation data.

In summary, nanoDMT is promising for reducing side effects in the environment and at the same time promoting pest control, resulting in



**Fig. 5.** Embryonic and larval morphological changes found in the assessment of zebrafish toxicity – FET Test (OECD 236, 2013). On display are representative photographs of some of the effects observed in organisms from each group tested: a) DMT-96 h-LC<sub>10</sub> spinal deformity; b) DMT-96 h-LC<sub>20</sub> tail deformity and decrease in length; c) cDMT-72 h-LC<sub>30</sub> yolk sac edema; d) NP + DMT-96 h-LC<sub>10</sub> spinal/tail deformity; e) DMT-96 h-LC<sub>40</sub> pericardial edema; f) cDMT-96 h-LC<sub>30</sub> spinal deformity; g) DMT-96 h-LC<sub>50</sub> yolk sac edema; h) NP + DMT-24 h-LC<sub>20</sub> hypopigmentation; i) cDMT-48 h-LC<sub>10</sub> pericardial edema; j) DMT-72 h-LC<sub>40</sub> pericardial edema.

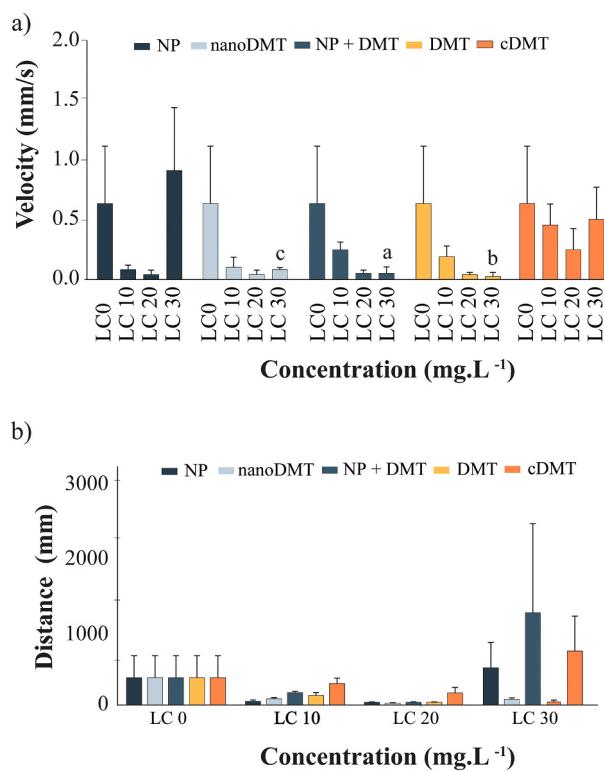


**Fig. 6.** Behavioral biomarkers in zebrafish larvae. a) Swimming speed evaluation ( $\text{mm} \cdot \text{s}^{-1}$ ) and b) distance covered (mm) of 96 hpf zebrafish larvae after exposure to NP, nanoDMT, NP + DMT, DMT and cDMT at different concentrations: LC<sub>0</sub> (control), LC<sub>10</sub>, LC<sub>20</sub> and LC<sub>30</sub> ( $\text{mg} \cdot \text{L}^{-1}$ ). Tests were performed with DanioVision equipment and analyzed by EthovisionXT (Noldus®) software for 10 min at 28 °C, where  $n = 36$  larvae/concentration. The statistical test was determined by two-way ANOVA followed by the Bonferroni test,  $p < 0.05$ . Different letters correspond to significant variations.

sustainability.

#### CRediT authorship contribution statement

**José Henrique Vallim:** Conceptualization, Writing – original draft, Writing – review & editing. **Zaira Clemente:** Conceptualization, Writing – review & editing. **Rodrigo Fernandes Castanha:** Conceptualization, Writing – review & editing. **Anderson do Espírito Santo Pereira:** Conceptualization, Writing – review & editing. **Estefânia Vangelie Ramos Campos:** Writing – review & editing, Supervision. **Márcia Regina Assalin:** Writing – review & editing, Supervision. **Cláudia Vianna Maurer-Morelli:** Writing – review & editing, Supervision. **Leonardo Fernandes Fraceto:** Conceptualization, Writing – review & editing, Supervision. **Vera Lúcia Scherholz Salgado de Castro:** Conceptualization, Writing – review & editing, Supervision.

#### Declaration of Competing Interest

The authors declare that they have no known competing financial interests or personal relationships that could have appeared to influence the work reported in this paper.

#### Acknowledgments

Authors would like to thank Embrapa, project number 01.14.03.001.02 – Nanotechnology applied to agribusiness, São Paulo Research Foundation (FAPESP #2017/21004-5) and National Council for Scientific and Technological Development (CNPq (405623/2018-6). A.E.S.P is grateful for a post-doctoral grant provided by CAPES-

Coordination for the Improvement of Higher Education Personnel (CAPES-PRINT project #88887.570381/2020-00).

#### Appendix A. Supplementary data

Supplementary data to this article can be found online at <https://doi.org/10.1016/j.impact.2022.100408>.

#### References

- Abou-Saleh, H., Younes, N., Rasool, K., Younis, M.H., Prieto, R.M., Yassine, H.M., Mahmoud, K.A., Pintus, G., Nasrallah, G.K., 2019. Impaired liver size and compromised neurobehavioral activity are elicited by chitosan nanoparticles in the Zebrafish embryo model. *Nanomaterials* 9, 122. <https://doi.org/10.3390/nano9010122>.
- Adisa, I.O., Pullagural, V.L.R., Peralta-Vide, J.R., Dimkpa, C.O., Elmer, W.H., Gardea-Torresdey, J.L., White, J.C., 2019. Recent advances in nano-enabled fertilizers and pesticides: a critical review of mechanisms of action. *Environ. Sci.: Nano* 6, 2002–2030. <https://doi.org/10.1039/C9EN00265K>.
- Ahmad, F., Noldus, L., Tegelenbosch, R., Richardson, M., 2012. Zebrafish embryos and larvae in behavioural assays. *Behaviour* 149, 1241–1281. <https://doi.org/10.1163/1568539X-00003020>.
- Aldridge, J.E., Levin, E.D., Seidler, F.J., Slotkin, T.A., 2005. Developmental exposure of rats to chlorpyrifos leads to behavioral alterations in adulthood, involving serotonergic mechanisms and resembling animal models of depression. *Environ. Health Perspect.* 113, 527–531. <https://doi.org/10.1289/ehp.7867>.
- Camara, M.C., Campos, E.V.R., Monteiro, R.A., do Espírito Santo Pereira, A., de Freitas Proença, P.L., Fraceto, L.F., 2019. Development of stimuli-responsive nano-based pesticides: emerging opportunities for agriculture. *J. Nanobiotechnol.* 17, 100. <https://doi.org/10.1186/s12951-019-0533-8>.
- Chakraborty, C., Sharma, A.R., Sharma, G., Lee, S.-S., 2016. Zebrafish: a complete animal model to enumerate the nanoparticle toxicity. *J. Nanobiotechnol.* 14, 65. <https://doi.org/10.1186/s12951-016-0217-6>.
- Chaud, M., Souto, E.B., Zielinska, A., Severino, P., Batain, F., Oliveira-Junior, J., Alves, T., 2021. Nanopesticides in agriculture: benefits and challenge in agricultural productivity, toxicological risks to human health and environment. *Toxics* 9, 131. <https://doi.org/10.3390/toxics9060131>.
- Chen, T., Li, S., Zhu, W., Liang, Z., Zeng, Q., 2019. Self-assembly pH-sensitive chitosan/alginate coated polyelectrolyte complexes for oral delivery of insulin. *J. Microencapsul.* 36 (1), 96–107. <https://doi.org/10.1080/02652048.2019.1604846>.
- Chen, L., Lin, Y., Zhou, H., Hao, L., Chena, H., Zhoua, X., 2021. A stable polyamine-modified zein-based nanoformulation with high foliar affinity and lowered toxicity for sustained avermectin release. *Pest Manag. Sci.* 77 (7), 3300–3312. <https://doi.org/10.1002/ps.6374>.
- Clemente, Z., Silva, G.H., Nunes, M.S.C., Martinez, D.S.T., Maurer-Morelli, C.V., Thomaz, A.A., Castro, V.L., 2019. Exploring the mechanisms of graphene oxide behavioral and morphological changes in zebrafish. *Environ. Sci. Pollut. Res.* 26 (29), 30508–30523. <https://doi.org/10.1007/s11356-019-05870-z>.
- Čolović, M.B., Krstić, D.Z., Lazarević-Pašti, T.D., Bondžić, A.M., Vasić, V.M., 2013. Acetylcholinesterase inhibitors: pharmacology and toxicology. *Curr. Neuropharmacol.* 11, 315–335. <https://doi.org/10.2174/1570159X11311030006>.
- Danaei, M., Dehghankhond, M., Ataei, S., Hasanzadeh Davarani, F., Javanmaard, R., Dokhani, A., Khorasani, S., Mozafari, M.R., 2018. Impact of particle size and polydispersity index on the clinical applications of lepidic nanocarrier systems. *Pharmaceutics* 10 (2), 1–17. <https://doi.org/10.3390/pharmaceutics10020057>.
- Dogan, D., Can, C., Kocayigit, A., Dikilitas, M., Taskin, A., Bilinc, H., 2011. Dimethoate-induced oxidative stress and DNA damage in *Oncorhynchus mykiss*. *Chemosphere* 84 (1), 39–46. <https://doi.org/10.1016/j.chemosphere.2011.02.087>.
- Duhan, J.S., Kumar, R., Kumar, N., Kaur, P., Nehra, K., Duhan, S., 2017. Nanotechnology, the new perspective in precision agriculture. *Biotechnol. Rep.* 15, 11–23. <https://doi.org/10.1016/j.btre.2017.03.002>.
- Eddins, D., Cerutti, D., Williams, P., Linney, E., Levin, E., 2010. Zebrafish provide a sensitive model of persisting neurobehavioral effects of developmental chlorpyrifos exposure, comparison with nicotine and pilocarpine effects and relationship to dopamine deficits. *Neurotoxicol. Teratol.* 32, 99–108. <https://doi.org/10.1016/j.nt.2009.02.005>.
- Fraysse, B., Mons, R., Garric, J., 2006. Development of a zebrafish 4-day embryo-larval bioassay to assess toxicity of chemicals. *Ecotoxicol. Environ. Saf.* 63 (2), 253–267. <https://doi.org/10.1016/j.ecoenv.2004.10.015>.
- Hertel, A.G., Niemela, P.T., Dingemanse, N.J., Mueller, T., 2020. A guide for studying among-individual behavioral variation from movement data in the wild. *Movement Ecol.* 8, 30. <https://doi.org/10.1186/s40462-020-00216-8>.
- Hertz-Pannier, I., Sassi, J.B., Engel, S., Bennett, D.H., Bradman, A., Eskenazi, B., Lanphear, B., Whyatt, R., 2018. Organophosphate exposures during pregnancy and child neurodevelopment: recommendations for essential policy reforms. *PLoS Med.* 15 (10), e1002671. <https://doi.org/10.1371/journal.pmed.1002671>.
- Hill, A.J., Bello, S.M., Prasch, A.L., Peterson, R.E., Heideman, W., 2004. Water permeability and TCDD-induced edema in zebrafish early-life stages. *Toxicol. Sci.* 78 (1), 78–87. <https://doi.org/10.1093/toxsci/kfh056>.
- Iavicoli, I., Leso, V., Beezhold, D.H., Shvedova, A.A., 2017. Nanotechnology in agriculture, opportunities, toxicological implications, and occupational risks.

- Toxicol. Appl. Pharmacol. 329, 96–111. <https://doi.org/10.1016/j.taap.2017.05.025>.
- Janeczek, M., Gefen, T., Samimi, M., Kim, G., Weintraub, S., Bigio, E., Rogalski, E., Mesulam, M.M., Geula, C., 2017. Variations in acetylcholinesterase activity within human cortical pyramidal neurons across age and cognitive trajectories. *Cereb. Cortex* 1, 1–9. <https://doi.org/10.1093/cercor/bhx047>.
- Jin, Y., Liu, Z., Peng, T., Fu, Z., 2015. The toxicity of chlorpyrifos on the early life stage of zebrafish, a survey on the endpoints at development, locomotor behavior, oxidative stress and immunotoxicity. *Fish. Shellfish Immunol.* 43, 405–414. <https://doi.org/10.1016/j.fsi.2015.01.010>.
- Kah, M., Kookana, R.S., Gogos, A., Bucheli, T.D., 2018. A critical evaluation of nanopesticides and nanofertilizers against their conventional analogues. *Nat. Nanotechnol.* 13, 677–684. <https://doi.org/10.1038/s41565-018-0131-1>.
- Katsikantami, I., Colosio, C., Alegakis, A., Tsatsarakis, M.N., Vakonaki, E., Rizos, A.K., Sarigiannis, D.A., Tsatsakis, A.M., 2019. Estimation of daily intake and risk assessment of organophosphorus pesticides based on biomonitoring data - the internal exposure approach. *Food Chem. Toxicol.* 123, 57–71. <https://doi.org/10.1016/j.fct.2018.10.047>.
- Khandelwal, N., Barbole, R.S., Banerjee, S.S., Chate, G.P., Biradar, A.V., Khandare, J.J., Giri, A.P., 2016. Budding trends in integrated pest management using advanced micro- and nano-materials, challenges and perspectives. *J. Environ. Manag.* 184, 157–169. <https://doi.org/10.1016/j.jenvman.2016.09.071>.
- Kumar, S., Bhanjana, G., Sharma, A., Dilbaghi, N., Sidhu, M.C., Kim, K.H., 2017. Development of nanoformulation approaches for the control of weeds. *Sci. Total Environ.* 586, 1272–1278. <https://doi.org/10.1016/j.scitotenv.2017.02.138>.
- Kumar, S., Nehra, M., Dilbaghi, N., Marrazza, G., Hassan, A., Kim, K.H., 2019. Nano-based smart pesticide formulations, emerging opportunities for agriculture. *J. Control. Release* 294, 131–153. <https://doi.org/10.1016/j.jconrel.2018.12.012>.
- Levin, E.D., Swain, H.A., Donerly, S., Linney, E., 2004. Developmental chlorpyrifos effects on hatchling zebrafish swimming behavior. *Neurotoxicol. Teratol.* 26, 719–723. <https://doi.org/10.1016/j.ntt.2004.06.013>.
- Li, L.L., Xu, Z., Kah, M., Lin, D., Filser, J., 2019. Nanopesticides: a comprehensive assessment of environmental risk is needed before widespread agricultural application. *Environ. Sci. Technol.* 53, 7923–7924. <https://doi.org/10.1021/acs.est.9b03146>.
- Lombi, E., Donner, E., Dusinska, M., Wickson, F.A., 2019. A one health approach to managing the applications and implications of nanotechnologies in agriculture. *Nat. Nanotechnol.* 14 (6), 523–531. <https://doi.org/10.1038/s41565-019-0460-8>.
- Loquercio, A., Castell-Perez, E., Gomes, C., Moreira, R.G., 2015. Preparation of chitosan-alginate nanoparticles for trans-cinnamaldehyde entrapment. *J. Food Sci.* 80 (10), N2305–N2315. <https://doi.org/10.1111/1750-3841.12997>.
- Lowry, G.V., Gregory, K.B., Apte, S.C., Lead, J.R., 2012. Transformations of nanomaterials in the environment. *Environ. Sci. Technol.* 46 (13), 6893–6899. <https://doi.org/10.1021/es300839e>.
- Lu, Z., Zhang, C., Gao, Y., Wang, W., Lin, J., Du, F., 2021. Simple, effective, and energy-efficient strategy to construct a stable pesticide nanodispersion. *ACS Agricul. Sci. Technol.* 1 (4), 329–337. <https://doi.org/10.1021/acscsитеch.1c00018>.
- Luo, Y., Wang, Q., Zhang, Y., 2020. Biopolymer-based nanotechnology approaches to deliver bioactive compounds for food applications: a perspective on the past, present, and future. *J. Agric. Food Chem.* 68 (46), 12993–13000. <https://doi.org/10.1021/acs.jafc.0c00277>.
- Majewski, M., Kasica, N., Jakimiuk, A., Podlasz, P., 2018. Toxicity and cardiac effects of acute exposure to tryptophan metabolites on the kynureneine pathway in early developing zebrafish (*Danio rerio*) embryos. *Toxicol. Appl. Pharmacol.* 341, 16–29. <https://doi.org/10.1016/j.taap.2018.01.004>.
- Mesallam, D.I.A., Hamid, O.I.A., Ibrahim, N.E., 2018. Ethanolic extract of fenugreek seeds moderates dimethoate-induced pancreatic damage in male rats. *Environ. Sci. Pollut. Res.* 25, 3894–3904. <https://doi.org/10.1007/s11356-017-0749-9>.
- Nazir, S., Ali, M.N., Tantry, J.A., Baba, I.A., Jan, A., Popescu, S.M., Paray, B.A., Gulnaz, A., 2022. Study of ultrastructural abnormalities in the renal cells of *Cyprinus carpio* induced by toxicants. *Toxics* 10, 177. <https://doi.org/10.3390/toxics10040177>.
- OECD. Organisation for Economic Co-operation and Development, 1992. Test No.203: Fish, acute toxicity test. In: OECD Guidelines for the Testing of Chemicals. Paris, France.
- OECD. Organisation for Economic Co-operation and Development, 2013. Test No.236: Fish Embryo Acute Toxicity (FET) Test. OECD Guidelines for the Testing of Chemicals. Paris, France.
- Park, H., Lee, J.Y., Park, S., Song, G., Lim, W., 2020. Developmental toxicity of fipronil in early development of zebrafish (*Danio rerio*) larvae: disrupted vascular formation with angiogenic failure and inhibited neurogenesis. *J. Hazard. Mater.* 385, 121531. <https://doi.org/10.1016/j.jhazmat.2019.121531>.
- Pereira, A.E.S., Silva, P.M., Oliveira, J.L., Oliveira, H.C., Fraceto, L.F., 2017. Chitosan nanoparticles as carrier systems for the plant growth hormone gibberellic acid. *Colloids Surf. B: Biointerfaces* 150, 141–152. <https://doi.org/10.1016/j.colsurfb.2016.11.027>.
- Pereira, B.V.R., Silva-Zacarin, E.C.M., Costa, M.J., dos Santos, A.C., do Carmo, J.B., Nunes, B., 2019. Cholinesterases characterization of three tropical fish species, and their sensitivity towards specific contaminants. *Ecotoxicol. Environ. Saf.* 173, 482–493. <https://doi.org/10.1016/j.ecoenv.2019.01.105>.
- Qiang, L., Cheng, J., Yi, J., Rotchell, J.M., Zhu, X., Zhou, J., 2016. Environmental concentration of carbamazepine accelerates fish embryonic development and disturbs larvae behavior. *Ecotoxicology* 25, 1426–1437. <https://doi.org/10.1007/s10646-016-1694-y>.
- Rani, S., Sud, D., 2022. Degradation of dimethoate pesticide in soil: impact of soil moisture and enhanced sunlight intensity. *Water Air Soil Pollut.* 233, 24. <https://doi.org/10.1007/s11270-021-05463-y>.
- Richendrfer, H., Creton, R., 2015. Chlorpyrifos and malathion have opposite effects on behaviors and brain size that are not correlated to changes in AChE activity. *NeuroToxicology* 49, 50–58. <https://doi.org/10.1016/j.neuro.2015.05.002>.
- Roy, N.M., Zambrzycka, E., Santangelo, J., 2017. Butyl benzyl phthalate (BBP) induces caudal defects during embryonic development. *Environ. Toxicol. Pharmacol.* 56, 129–135. <https://doi.org/10.1016/j.etap.2017.09.009>.
- Sarmento, B., Ferreira, D., Veiga, F., Ribeiro, A., 2006. Characterization of insulin-loaded alginate nanoparticles produced by ionotropic pre-gelation through DSC and FTIR studies. *Carbohydr. Polym.* 66 (1), 1–7. <https://doi.org/10.1016/j.carbpol.2006.02.008>.
- Schmitt, C., McManus, M., Kumar, N., Awoyemi, O., Crago, J., 2019. Comparative analyses of the neurobehavioral, molecular, and enzymatic effects of organophosphates on embryo-larval zebrafish (*Danio rerio*). *Neurotoxicol. Teratol.* 73, 67–75. <https://doi.org/10.1016/j.ntt.2019.04.002>.
- Schwalbe, M.A.B., Boden, A.L., Wise, T.N., Tytell, E.D., 2019. Red muscle activity in bluegill sunfish *Lepomis macrochirus* during forward accelerations. *Sci. Rep.* 9 (1), 8088. <https://doi.org/10.1038/s41598-019-44409-7>.
- Sharma, N., Madan, P., Lin, S., 2016. Effect of process and formulation variables on the preparation of parenteral paclitaxel-loaded biodegradable polymeric nanoparticles: A co-surfactant study. *Asian J. Pharmaceut. Sci.* 11 (3), 404–416. <https://doi.org/10.1016/j.ajps.2015.09.004>.
- Shaw, B.J., Liddle, C.C., Windeatt, K.M., Handy, R.D., 2016. A critical evaluation of the fish early life stage toxicity test for engineered nanomaterials, experimental modifications and recommendations. *Arch. Toxicol.* 90, 2077–2107. <https://doi.org/10.1007/s00204-016-1734-7>.
- Siepmann, J., Peppas, N.A., 2001. Modeling of drug release from delivery systems based on hydroxypropyl methylcellulose (HPMC). *Adv. Drug Deliv. Rev.* 48 (2–3), 139–157. [https://doi.org/10.1016/S0169-409X\(01\)00112-0](https://doi.org/10.1016/S0169-409X(01)00112-0).
- Slattery, M., Harper, B., Harper, S., 2019. Pesticide encapsulation at the nanoscale drives changes to the hydrophobic partitioning and toxicity of an active ingredient. *Nanomaterials* 9 (1), 81. <https://doi.org/10.3390/nano9010081>.
- Sousa, J.C.G., Ribeiro, A.R., Barbosa, M.O., Pereira, M.F.R., Silva, A.M.T., 2018. A review on environmental monitoring of water organic pollutants identified by EU guidelines. *J. Hazard. Mater.* 344, 146–162. <https://doi.org/10.1016/j.jhazmat.2017.09.058>.
- Thai, H., Thuy Nguyen, C., Thi Thach, L., Tran, M.T., Mai, H.D., Nguyen, T.T.T., Le, G.D., Can, M.V., Tran, L.D., Bach, G.L., Ramadass, K., Sathish, C.I., Le, Q.V., 2020. Characterization of chitosan/alginate/lovastatin nanoparticles and investigation of their toxic effects *in vitro* and *in vivo*. *Sci. Rep.* 10, 909. <https://doi.org/10.1038/s41598-020-57666-8>.
- Thanh, N.T.K., Maclean, N., Mahiddine, S., 2014. Mechanisms of nucleation and growth of nanoparticles in solution. *Chem. Rev.* 114 (15), 7610–7630. <https://doi.org/10.1021/cr400544s>.
- Tierney, K., Casselman, M., Takeda, S., Farrell, T., Kennedy, C., 2007. The relationship between cholinesterase inhibition and two types of swimming performance in chlorpyrifos-exposed coho salmon (*Oncorhynchus kisutch*). *Environ. Toxicol. Chem.* 26 (5), 998–1004. <https://doi.org/10.1897/06-459r.1>.
- Toledo-Ibarra, G.A., Rodríguez-Sánchez, E.J., Ventura-Ramón, H.G., Díaz-Resendiz, K.J.G., Girón-Pérez, M.I., 2018. Cholinergic alterations by exposure to pesticides used in control vector: guppies fish (*Poecilia reticulata*) as biological model. *Int. J. Environ. Health Res.* 28 (1), 79–89. <https://doi.org/10.1080/09603123.2018.1429577>.
- Triassi, M., Nardone, A., Giovinetti, M.C., De Rosa, E., Canzanella, S., Sarnacciaro, P., Montuori, P., 2019. Ecological risk and estimates of organophosphate pesticides loads into the Central Mediterranean Sea from Volturino River, the river of the “Land of Fires” area, southern Italy. *Sci. Total Environ.* 678, 741–754. <https://doi.org/10.1016/j.scitotenv.2019.04.202>.
- USEPA, 2002. Methods for Measuring the Acute Toxicity of Effluents and Receiving Waters to Freshwater and Marine Organisms. Fifth edition, Washington.
- Vurro, M., Miguel-Rojas, C., Pérez-de-Luque, A., 2019. Safe nanotechnologies for increasing the effectiveness of environmentally friendly natural agrochemicals. *Pest Manag. Sci.* 75 (9), 2403–2412. <https://doi.org/10.1002/ps.5348>.
- Walker, G.W., Kookana, R.S., Smith, N.E., Kah, M., Doolittle, C.L., Reeves, P.T., Lovell, W., Anderson, D.J., Turney, T.W., Navarro, D.A., 2018. Ecological risk assessment of nano-enabled pesticides: a perspective on problem formulation. *J. Agric. Food Chem.* 66 (26), 6480–6486. <https://doi.org/10.1021/acs.jafc.7b02373>.
- Wang, C., Cui, B., Wang, Y., Wang, M., Zeng, Z., Gao, F., Sun, C., Guo, L., Zhao, X., Cui, H., 2021a. Preparation and size control of efficient and safe nanopesticides by anodic aluminum oxide templates-assisted method. *Int. J. Mol. Sci.* 22, 8348. <https://doi.org/10.3390/ijms22158348>.
- Wang, J., Teng, Y., Zhai, Y., Yue, W., Pan, Z., 2021b. Spatiotemporal distribution and risk assessment of organophosphorus pesticides in surface water and groundwater on the North China Plain, China. *Environ. Res.* 112310. <https://doi.org/10.1016/j.envres.2021.112310>.
- Watson, F.L., Schmidt, H., Turman, Z.K., Hole, N., Garcia, H., Gregg, J., Tilghman, J., Fradinger, E.A., 2014. Organophosphate pesticides induce morphological abnormalities and decrease locomotor activity and heart rate in *Danio rerio* and *Xenopus laevis*. *Environ. Toxicol. Chem.* 33 (6), 1337–1345. <https://doi.org/10.1002/etc.2559>.
- Wilson, K.S., Matrone, G., Livingstone, D.E., Al-Dujaili, E.A., Mullins, J.J., Tucker, C.S., Hadoke, P.W., Kenyon, C.J., Denir, M.A., 2013. Physiological roles of glucocorticoids during early embryonic development of the zebrafish (*Danio Rerio*). *J. Physiol.* 591, 6209–6220. <https://doi.org/10.1113/jphysiol.2013.256826>.

- Wu, Y., Zhang, Y., Chen, M., Yang, Q., Zhuang, S., Lv, L., Zuo, Z., Wang, C., 2019. Exposure to low-level metalaxyl impacts the cardiac development and function of zebrafish embryos. *J. Environ. Sci. (China)* 85, 1–8. <https://doi.org/10.1016/j.jes.2019.03.019>.
- Zhao, X., Cui, H., Wang, Y., Sun, C., Cui, B., Zeng, Z., 2018. Development strategies and prospects of nano-based smart pesticide formulation. *J. Agric. Food Chem.* 66 (26), 6504–6512. <https://doi.org/10.1021/acs.jafc.7b02004>.
- Zohri, M., Akbari Javar, H., Gazori, T., Khoshayand, M.R., Aghaei-Bakhtiari, S.H., Gahremani, M.H., 2020. Response surface methodology for statistical optimization of chitosan/alginate nanoparticles as a vehicle for recombinant human bone morphogenetic protein-2 delivery. *Int. J. Nanomedicine* 15, 8345–8356. <https://doi.org/10.2147/IJN.S250630>.